IOP PUBLISHING JOURNAL OF PHYSICS D: APPLIED PHYSICS

J. Phys. D: Appl. Phys. **41** (2008) 185107 (5pp) doi:10.1088/0022-3727/41/18/185107

Fabrication of heterojunction solar cells by using microcrystalline hydrogenated silicon oxide film as an emitter

Chandan Banerjee[1,3], Jaran Sritharathikhun[1], Akira Yamada[2] and Makoto Konagai[1]

[1] Department of Physical Electronics, Tokyo Institute of Technology, 2-12-1-S9-9 O-okayama, Meguro-ku, Tokyo 152-8552, Japan
[2] Quantum Nanoelectronics Research Center, Tokyo Institute of Technology, 2-12-1-S9-9 O-okayama, Meguro-ku, Tokyo 152-8552, Japan

E-mail: chandu_phy2004@yahoo.co.in

Received 12 April 2008, in final form 14 July 2008
Published 29 August 2008
Online at stacks.iop.org/JPhysD/41/185107

Abstract

Wide gap, highly conducting n-type hydrogenated microcrystalline silicon oxide (μc-SiO : H) films were prepared by very high frequency plasma enhanced chemical vapour deposition at a very low substrate temperature (170 °C) as an alternative to amorphous silicon (a-Si : H) for use as an emitter layer of heterojunction solar cells. The optoelectronic properties of n-μc-SiO : H films prepared for the emitter layer are dark conductivity = 0.51 S cm^{-1} at 20 nm thin film, activation energy = 23 meV and E_{04} = 2.3 eV. Czochralski-grown 380 μm thick p-type ⟨1 0 0⟩ oriented polished silicon wafers with a resistivity of 1–10 Ω cm were used for the fabrication of heterojunction solar cells. Photovoltaic parameters of the device were found to be V_{oc} = 620 mV, J_{sc} = 32.1 mA cm^{-2}, FF = 0.77, η = 15.32% (active area efficiency).

1. Introduction

An amorphous or microcrystalline heterojunction with crystalline silicon is a promising candidate for highly efficient solar cells processed at low temperatures. Sanyo, which reached 21%, already demonstrated the high potential of such a device on n-type Czochralski (CZ) Si substrates [1]. Inspired by the outstanding performance of the heterojunction with intrinsic thin (HIT) layer cells, dozens of research groups [2–6] throughout the world have been trying to duplicate Sanyo's results with only partial success so far, due to insufficient understanding of the hetero-interface and lack of open literature about critical surface pretreatments and other process steps. In addition, because p-type silicon is a more common photovoltaic (PV) material, single heterojunction (SHJ) cells on p-type c-Si are more popular than those on n-type. Today most groups are focusing on p-type substrates and recently 17.8% efficiency has been obtained on p-type FZ material [4]. While progress in p-type heterojunction cells is steady, simulation studies indicate that heterojunction solar cells on n-type material are intrinsically better than on p-type material because of the better band alignment [2, 7]. It therefore appears that for highly efficient solar cells, n-type material should be used. It is still an open question whether the heterojunction approach on p-type material can replace the standard p thermal diffusion for low cost industrial solar cells. However, considering the continually increasing efficiencies on p-type we are fabricating heterojunction solar cells on p-type wafers.

To develop an alternative to a-Si layers, we have initiated our research in the direction of fabricating HIT-type solar cells with microcrystalline silicon alloys such as μc-3C-SiC : H, μc-SiO : H. In our previous report we showed the application of n-type hydrogenated microcrystalline cubic silicon carbide (μc-3C-SiC : H) as an emitter [8]. High conductivity, wide optical gap and good surface passivation of the μc-SiO$_x$: H film encourage us to use it as an alternative to a-Si : H. Yablonovitch *et al* [9] showed a 720 mV open circuit voltage with an n$^+$-SIPOS–p-c-Si–n$^+$-SIPOS (semi-insulating polycrystalline silicon) double heterostructure solar cell, but the series resistance limited the fill factor to 0.5. They used SiO$_x$ as an SIPOS and the process temperature was very

[3] Author to whom any correspondence should be addressed.

Table 1. Deposition conditions of different films used in the device fabrication.

Type of film	Gases used	Gas flow (sccm)	Pressure (Torr)	$T_{Substrate}$ (°C)	Power (mW cm^{-2})
n-μc-SiO : H (Emitter)	$SiH_4/H_2/CO_2/PH_3$	3/180/1.8/2.5	0.5	170	20
a-SiO_x : H (Buffer)	$SiH_4/H_2/CO_2$	6/60/1.8	0.4	170	20
p-a-SiO : H	$SiH_4/H_2/CO_2/B_2H_6$	3/180/1.8/5	0.5	170	20

high. Outstanding voltage performance was possible due to the excellent bulk quality of the c-Si as well as excellent surface passivation of the n^+-SIPOS hetero-contact. In another report we have already showed the potential of low temperature deposited a-SiO_x : H films for surface passivation on the c-Si surface [10]. In this paper we will report the possible formation of heterojunction solar cells by depositing an n-type μc-SiO thin film by very high frequency plasma enhanced chemical vapour deposition (VHF-PECVD) at a very low substrate temperature (170 °C) on a p-type Si wafer. This is the first report on a heterojunction solar cell where μc-SiO : H is used as an emitter. The optoelectronic properties of the n-μc-SiO : H film prepared for an emitter layer of the heterojunction solar cell are dark conductivity = 0.51 S cm^{-1} at 20 nm thin film, activation energy = 23 meV and $E_{04} = 2.3$ eV. We also show the introduction of an ultra-thin a-SiO_x : H as a new type buffer layer at the front interface of the heterojunction.

2. Experimental details

n-type μc-SiO : H material was made by PECVD in a single chamber deposition system, excited by VHF (60 MHz) with a power density of 20 mW cm^{-2} at a very low substrate temperature (170 °C). A source gas mixture of high purity SiH_4 + H_2 + PH_3 + CO_2 has been used. Details of the deposition conditions are shown in table 1. For optical and electrical characterization, films were deposited on Corning 7059 glass and Si substrates. Spectroscopy ellipsometry (M-2000 UI, J.A. Woollam Co. Inc.) was used to determine the absorbance spectra and E_{04} (energy corresponding to the absorption coefficient $\sim 10^4$) in the visible spectral range. The bonding configuration within the film was characterized by Fourier transform infrared spectroscopy (FTIR; MAGNA-IR 760, Nicolet). The oxygen content of the film was calculated by x-ray photoelectron spectroscopy (XPS; JPS 9200, JEOL) and depth profile by secondary ion mass spectrometry (SIMS; ULVAC-PHI ADEPT1010) measurements. Samples were also examined by x-ray diffraction (XRD; X'Pert-MPD, Philips) and Raman scattering (RS-1000, JASCO) to determine the crystallinity. The temperature dependence of dark conductivity (σ_D) was measured using a pair of Al coplanar gap-cell electrodes. The activation energy (E_a) of the electric conductivity was deduced.

Commercial CZ-grown 380 μm thick p-type $\langle 1\,0\,0 \rangle$ oriented one side polished silicon wafers with a resistivity of 1–10 Ω cm were used to fabricate the heterojunction solar cell. The wafers received a standard RCA cleaning and dip in HF 5% to remove the native oxide.

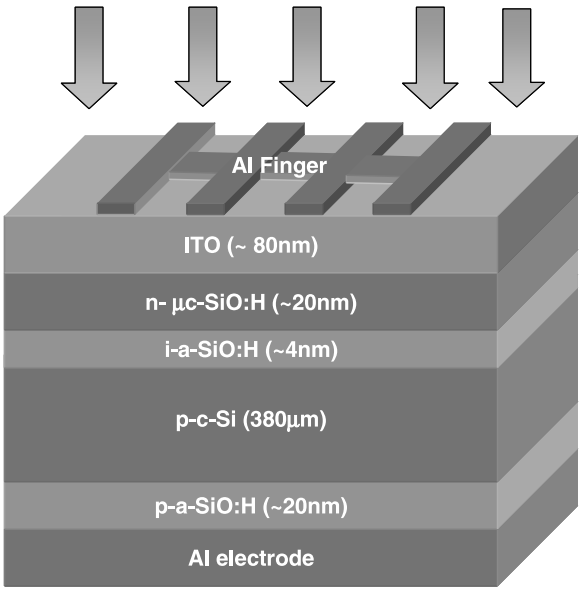

Figure 1. Structure of a solar cell fabricated by using n-μc-SiO : H as an emitter.

The heterojunctions were then fabricated by the successive deposition of the a-SiO : H buffer layer and n-μc-SiO : H as an emitter on the polished side of the silicon wafer. An ITO thin film was deposited by rf magnetron sputtering at a substrate temperature of 200 °C, followed by the deposition of aluminium fingers as the emitter contacts to complete the fabrication of the devices. p-a-SiO : H was deposited on the backside prior to the Al back contact to make a good ohmic contact. The structure of the device is shown in figure 1. Reactive ion etching (RIE) was carried out on the top side for mesa-etching. The active area of the solar cell was 0.23 cm^2. The solar cells were characterized by light current density–voltage (J–V; Agilent 4156C, Agilent) (AM 1.5, 100 mW cm^{-2}, 25 °C) and external quantum efficiency (YQ-250, JASCO) measurements. The front interface of the device with and without buffer layer was investigated by a high resolution cross-sectional transmission electron micrograph (TEM; H-9000NAR, Hitachi).

3. Results and discussions

First we will discuss the properties of the n-μc-SiO : H film deposited at a low substrate temperature. Figure 2 shows the Raman spectra of the films having thicknesses 150 nm and 20 nm, respectively. As we used 20 nm thick films for the emitter layer, we characterize the film at that thickness

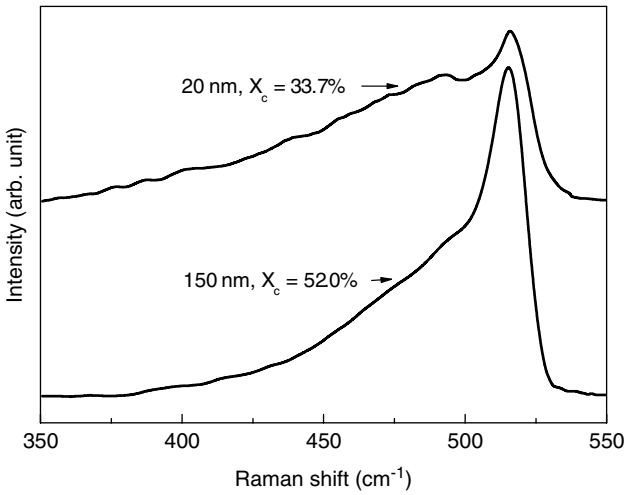

Figure 2. Raman spectra of the n-μc-SiO : H film deposited on glass (normalized at ∼520 cm^{-1}) having thicknesses of 150 nm and 20 nm.

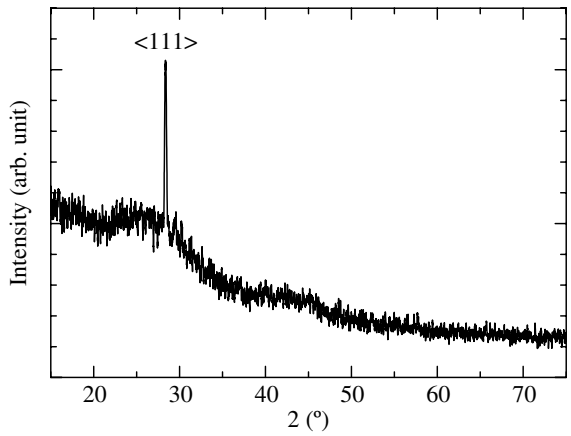

Figure 3. XRD pattern of the 150 nm thick n-μc-SiO : H film deposited on glass.

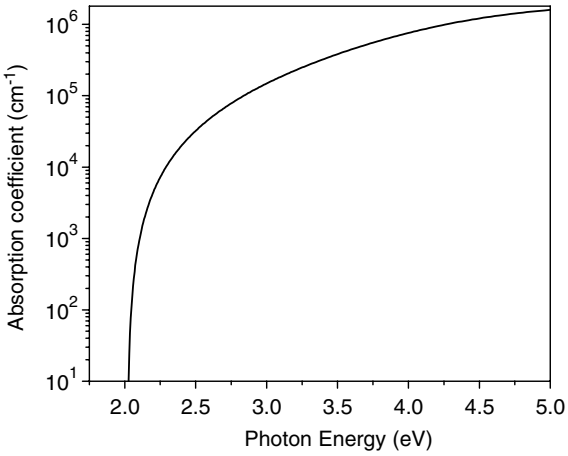

Figure 4. Absorption spectrum of the n-μc-SiO : H film measured by spectroscopic ellipsometry.

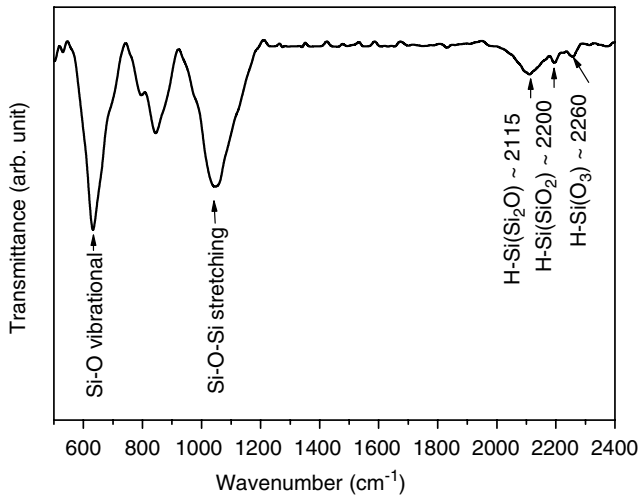

Figure 5. FTIR spectra of the 150 nm thick n-μc-SiO : H film deposited on c-Si showing different bonding configurations.

value. The crystalline volume fractions estimated from figure 2 were 52% and 33.7%, respectively. The XRD study of this sample shows a distinct peak at $2\theta = 28.4^\circ$ which corresponds to the $\langle 1\,1\,1\rangle$ plane of crystalline silicon (figure 3). The dark conductivity and activation energy were measured after depositing a coplanar aluminium electrode on the film grown on Corning 7059 glass. The activation energy was calculated from the slope of the Arhenius plot. The film at 20 nm thickness shows dark conductivity and activation energy of 0.51 S cm^{-1} and 23 meV, respectively. Absorption of the film was studied by spectroscopic ellipsometry. Figure 4 shows the absorption spectrum of the film. The Tauc model was used to fit the experimental data in spectroscopic ellipsometry. From the figure we can estimate that the E_{04} value (energy corresponding to the absorption coefficient ∼10^4) of the film is 2.3 eV, whereas the values of the band gap and dark conductivity for the conventional n-a-Si : H emitter found from the literature [11] are 1.70 eV and 1.9×10^{-2} S cm^{-1}, respectively. This high conductivity as well as high optical gap of the film compared with a conventional a-Si : H emitter encourages us to fabricate heterojunction solar cells by using this material as an emitter layer. According to Watanabe *et al* [12] SiO : H is a two-phase material with an island of SiO in a matrix of a-Si : H. In their two-phase model, the oxygen-rich phase is effective in increasing the optical gap and the Si-rich phase contributes to high conductivity. This is why the optical gap is high retaining higher conductivity. The oxygen content of the film was 8 at%, estimated from the XPS measurement. Figure 5 shows the FTIR spectra of the film. The bonded hydrogen content of the film was estimated to be 20 at%. According to the random-bonding model (RBM) [13] unhydrogenated silicon oxide films are composed of five basic bonding configurations: Si ($Si_{4-n}O_n$), n = 0–4. The basic bonding units are Si_2O, SiO, Si_2O_3 and SiO_2. Whereas in hydrogenated SiO_x : H films, according to the modified random-bonding model (MBR) the incorporation of Si–H bonds into the film can be performed by replacing an Si nearest neighbour to the Si site by an H atom in Si ($Si_{4-n}O_n$), n = 0–4 configurations [14], corresponding Si–H stretching absorption peaks associated with H–Si ($Si_{3-n}O_n$) configurations occur at 2000 cm^{-1}, 2115 cm^{-1}, 2200 cm^{-1} and 2260 cm^{-1} for n = 0, 1, 2 and 3, respectively. Usually 2000 cm^{-1} corresponds to

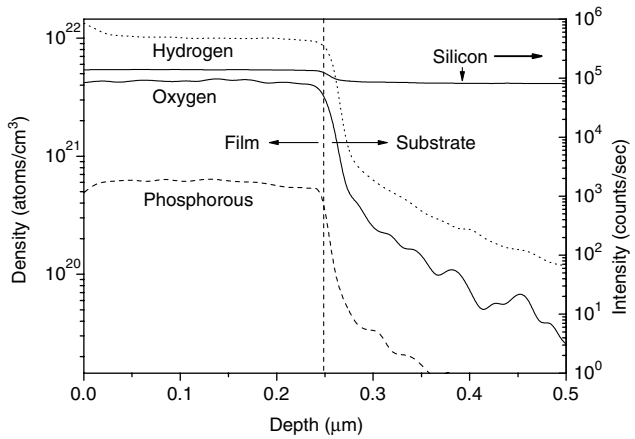

Figure 6. SIMS depth profile of the 250 nm thick n-μc-SiO : H film deposited on c-Si.

Table 2. PV parameters of device fabricated with and without buffer layer.

Solar cell structure	V_{oc} (V)	J_{sc} (mA cm^{-2})	FF	η (%)	Ideality factor (n)
Without buffer	0.56	32.9	0.71	13.08	1.43
With buffer	0.62	32.1	0.77	15.32	1.20

the SiH stretching mode. Due to oxygen attachment the peak shifts to a higher wavenumber. The SiH stretching absorption profile in figure 3 can be decomposed into three components at around 2115 cm^{-1}, 2200 cm^{-1} and 2260 cm^{-1}, i.e. peaks are for $n = 1$, 2 and 3, respectively. Figure 6 shows the SIMS depth profile of the 250 nm thick n-μc-SiO : H film for the density of oxygen, phosphorus and hydrogen in atoms cm^{-3}.

A heterojunction solar cell was then realized by using the aforesaid material as an emitter. First we optimized the heterostructure without inserting any intrinsic buffer layer at the front interface and the results are shown in table 2 along with the data with the buffer layer. We got an active area efficiency of 13.08% with the open circuit voltage (V_{oc}) as low as 560 mV and fill factor of 0.71. With the introduction of an ultra-thin (∼4 nm) intrinsic hydrogenated amorphous SiO as a front buffer layer at the p-c-Si and n-μc-SiO : H interface, V_{oc} improves by 60 mV. The fill factor also improves to 0.77. This may be due to the good surface passivation by the i-a-SiO : H film as well as the low interface defect density at the front interface owing to the deposition of a good quality buffer layer. With this interface improvement the active area efficiency increases to as high as 15.32% having V_{oc} of 620 mV. We performed a cross-sectional TEM study to investigate the front interface. Figures 7(*a*) and (*b*) show the cross-sectional TEM study of the front interface of the device with and without buffer, respectively. We estimated the thicknesses of the buffer and emitter layers from the cross-sectional TEM, which matches very well (3.5 nm and 19.4 nm) with the data estimated from the deposition rate of the respective films. From the figure it is clear that the interface becomes less rough when we use an ultra-thin buffer layer. This may be due to the low hydrogen dilution used during buffer deposition compared with high hydrogen dilution used

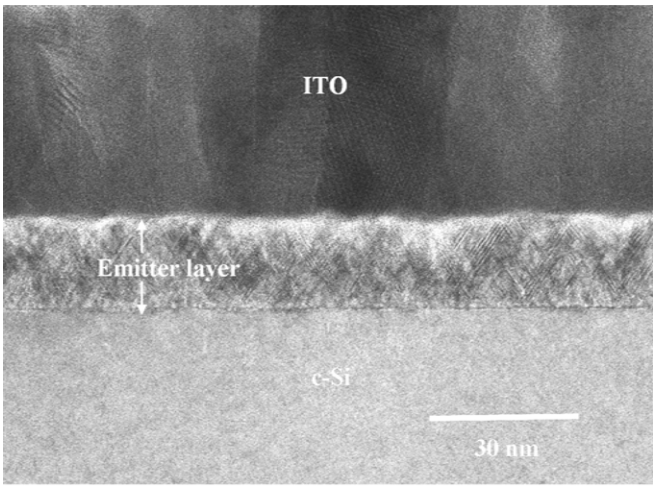

(a)

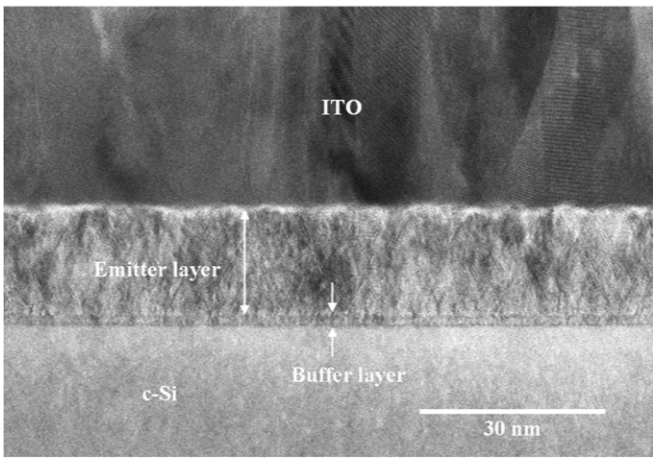

(b)

Figure 7. Cross-sectional TEM picture for the front interface of the device (*a*) without and (*b*) with an intrinsic buffer layer.

at μc-SiO : H emitter deposition directly because hydrogen plasma etching is one of the processes to etch the mono- and multi-crystalline silicon wafer [15]. This smooth interface with a buffer layer is another reason for the improvement in V_{oc} and FF along with excellent surface passivation by terminating the dangling bonds at the interface. Also the buffer layer separates the interface away from the doped (defective) layer. This is why the interface sits in the strong electric field and lowers the surface recombination velocity resulting in the improvement in V_{oc}. Here the smooth interface predominates over the small series resistance added by the ultra thin buffer layer, improving the FF. Figure 8 shows the illuminated J–V characteristic of the solar cells fabricated with and without a buffer layer along with the PV parameters for the same. From the figure it is clear that the series resistance is slightly higher for the cell fabricated without a buffer layer compared with that with a buffer layer resulting in a difference in the fill factor. The external quantum efficiency of the solar cells fabricated with and without a buffer layer is shown in figure 9. Solar cells fabricated without a buffer layer show better spectral response at the short wavelength region compared with the one fabricated with a ∼4 nm thick buffer layer. This result

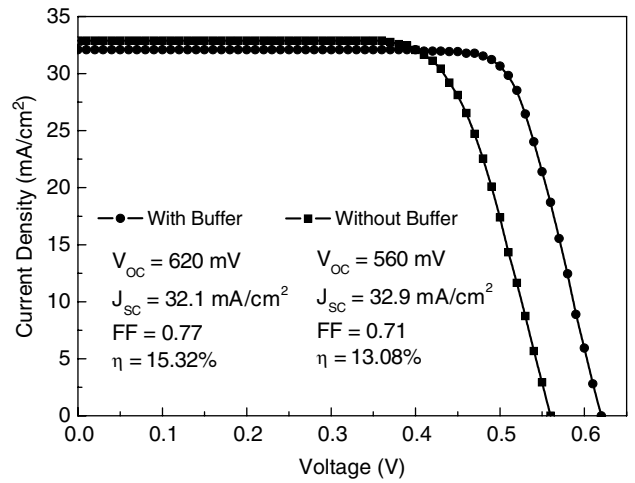

Figure 8. Illuminated I–V characteristics of the solar cells fabricated with and without a buffer layer.

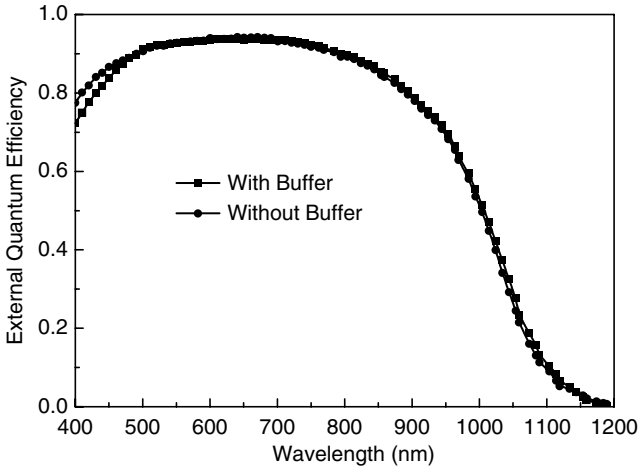

Figure 9. External quantum efficiency graph of the solar cells fabricated with and without a buffer layer.

is also reflected by the slightly higher short circuit current of the cells fabricated without a buffer layer compared with that with a buffer layer. It may be due to the small absorption by the buffer layer. The superiority of the wide bandgap n-μc-SiO : H film as the emitter layer has been established on the basis of the good spectral response at short wavelengths. However, the p-Si/p-a-SiO : H interface at the backside limits the spectral response at a higher wavelength due to the back-surface recombination.

4. Conclusions

The potential of the low temperature deposited, high conductivity (dark conductivity = 0.51 S cm^{-1} at 20 nm thin film), wide gap (E_{04} = 2.3 eV) n-type μc-SiO film as an emitter for heterojunction solar cells has been explored. Heterojunction solar cells have been made by using CZ-grown, ⟨1 0 0⟩ oriented, p-type, 380 μm thick Si wafers. The devices fabricated without inserting a thin intrinsic buffer layer showed an active area efficiency of about 13.08%. Introduction of a 4 nm thick intrinsic a-SiO$_x$: H buffer layer at the front interface improves the V_{oc} by 60 mV and also the active area efficiency to as high as 15.32%. Insertion of the buffer layer introduces some absorption at the lower wavelength region but improves the FF and V_{oc} by separating the interface away from the doped (defective) layer as well as lowering the surface recombination velocity. The use of a textured substrate may further increase the efficiency by enhancing the light trapping mechanism within the device.

Acknowledgment

This work is supported by the Japan Society for the Promotion of Science (JSPS).

References

[1] Maruyama E, Terakawa A, Taguchi M, Yoshimine Y, Ide D, Baba T, Shima M, Sakata H and Tanaka M 2006 *Proc. 4th World Conf. on Photovoltaic Energy Conversion (Hawaii, USA)* p 1455
[2] Jensen N, Hausner R M, Bergmann R B, Werner J H and Rau U 2002 *Prog. Photovolt.* **10** 1
[3] Roca F, Cárabe J, Jäger-Waldau A 2004 *19th European PV Solar Energy Conf. (Paris, France, 7–11 June)* p 1321
[4] Wang T H, Iwaniczko E, Page M R, Wang Q, Xu Y, Yan Y, Levi D, Roybal L, Bauer R and Branz H M 2006 *Proc. 4th World Conf. on Photovoltaic Energy Conversion (Hawaii, USA)* p 1439
[5] Tucci M, della Noce M, Bobeico E, Roca F, de Cesare G and Palma F 2004 *Thin Solid Films* **451–452** 355
[6] Zignani F, Desalvo A, Centurioni E, Iencinella D, Rizzoli R, Summonte C and Migliori A 2004 *Thin Solid Films* **451–452** 350
[7] Vukadinovic M, Cernivec G, Krc J, Agostinelli G, Goldbach H D, Schropp R E I, Smole F and Topic M 2004 *Proc. 19th European Photovoltaic Solar Energy Conf. (Paris, France)* p 773
[8] Banerjee C, Narayanan K L, Haga K, Sritharathikhun J, Miyajima S, Yamada A and Konagai M 2007 *Japan. J. Appl. Phys.* **46** 1
[9] Yablonovitch E, Gmitter T, Swanson R M and Kwark Y H 1985 *Appl. Phys. Lett.* **47** 1211
[10] Sritharathikhun J, Banerjee C, Otsubo M, Sugiura T, Yamamoto H, Sato T, Limmanee A, Yamada A and Konagai M 2007 *Japan. J. Appl. Phys.* **46** 3296
[11] Borchert D, Grabosch G and Fahrner W R 1997 *Sol. Energy Mater. Sol. Cells* **49** 53
[12] Watanabe H, Haga K and Lohner T 1993 *J. Non-Cryst. Solids* **164–166** 1085
[13] Phillip H R 1972 *J. Non-Cryst. Solids* **8–10** 627
[14] He L, Kurata Y, Inokuma T and Hasegawa S 1993 *Appl. Phys. Lett.* **63** 162
[15] Dhamrin M, Ghazali N H, Jeon M S, Saitoh T and Kamisako K 2006 *Proc. 4th World Conf. on Photovoltaic Energy Conversion (Hawaii, USA)* p 1395